

# On the correlation functions of the domain wall six vertex model\*

Omar Foda<sup>1</sup> and Ian Preston<sup>2</sup>

<sup>1</sup>Department of Mathematics and Statistics,  
The University of Melbourne,  
Parkville, Victoria 3010, Australia.

<sup>2</sup>Magdalen College,  
Oxford, OX1 4AU, Oxfordshire, UK

August 14, 2018

## Abstract

We propose an (essentially combinatorial) approach to the correlation functions of the domain wall six vertex model.

We reproduce the boundary 1-point function determinant expression of Bogoliubov, Pronko and Zvonarev, then use that as a building block to obtain analogous expressions for boundary 2-point functions.

The latter can be used, at least in principle, to express more general boundary (and bulk) correlation functions as sums over (products of) determinants.

## 1 Introduction

Computing off critical correlation functions<sup>1</sup> is probably the most challenging open problem currently under investigation in exactly solvable lattice models [1].

The six vertex model, with domain wall boundary conditions (dwbc's) is an ideal testing ground of possible approaches to such computations, particularly if one is interested in computations on a finite lattice<sup>2</sup>.

The model was first introduced by Korepin [2], who also formulated recursion relations that uniquely determine the partition function. Korepin's recursion relations were solved by Izergin [3], who obtained a determinant representation for the partition function.

---

\*Supported by the Australian Research Council (ARC).

<sup>1</sup>The literature on off critical correlation functions is extensive. We refer the reader to [4] for references to the literature up to the early 90's and to a search of <http://arXiv.org> for more recent literature.

<sup>2</sup>The previous footnote applies *verbatim* to the literature on the domain wall six vertex model.

Using the algebraic Bethe *ansatz* [4], Bogoliubov, Pronko and Zvonarev introduced a definition of boundary 1-point functions in the model [5], and computed them in determinant form<sup>3</sup>.

Inspired by Bogoliubov *et al*, we propose a definition of boundary  $n$ -point functions, that in the specific case that they considered, (almost) coincides with theirs (up to obvious factors due to the differences in our definitions of what a boundary 1-point function is).

We use combinatorics, based on the Yang Baxter equation, to compute determinant representations for boundary 1-point, and 2-point functions, and outline the (almost mechanical) extension to (certain) boundary  $n$ -point and bulk correlation functions. In the case of boundary 1-point functions, we reproduce the result of Bogoliubov *et al* [5] using elementary manipulations.

Our derivations are (basically) combinatorial and rely on repeated application of graphical operations, hence the proliferation of figures in the paper<sup>4</sup>.

There has been interest in this very model from algebraic combinatorialists over the past decade, particularly since the work of Kuperberg [6]. Our exposition is elementary in the hope that it will serve as an introduction to this part of exactly solved statistical mechanical models for non-physicists.

## 2 The model

To be reasonably self-contained, we start by recalling basic definitions related to lattice models in general, and to the dwbc six vertex model in particular. We refer the reader to [1, 4] for further details.

**Lattice configurations** Consider a square lattice, with  $N_c$  vertical lines (columns) labeled *from left to right* as  $\{N_c, N_c - 1, \dots, 2, 1\}$ , and  $N_r$  horizontal lines (rows) labeled *from top to bottom* as  $\{1, 2, \dots, N_r - 1, N_r\}$ . Initially, we take  $N_c = N_r = N$ . Later, we will relax this condition and consider lattices with deviations from dwbc's and  $N_c \neq N_r$ .

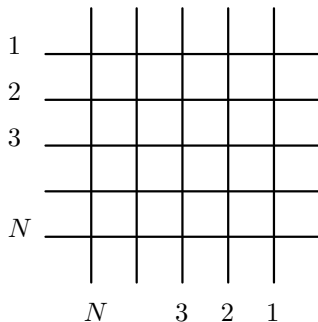


**Figure 1** *Our playing field*

<sup>3</sup>Bogoliubov *et al* obtained determinant expressions for the 1-point functions, and also for the boundary spontaneous polarization, which is a more difficult problem. Here, we discuss only the former.

<sup>4</sup>Our results can be produced using the algebraic Bethe *ansatz*. However, our method is elementary, and hopefully there is virtue in having more than one approach to this problem.

**Boundary lines** or simply ‘boundaries’, are the right most, left most, top and bottom lattice lines.

**Orientations** We assign each lattice line an orientation. In our convention, horizontal lines are oriented *from left to right*. Vertical lines are oriented *from bottom to top*.

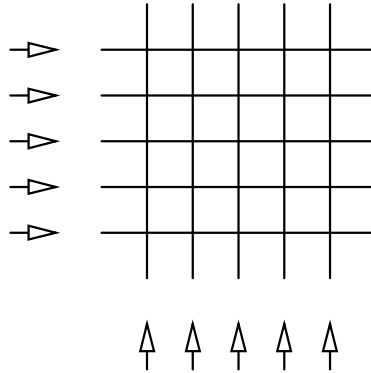


**Figure 2** The white arrows denote the orientations of the lattice lines.

**Rapidities** We assign each oriented lattice line a complex variable called a rapidity. We assign the  $i$ -th horizontal line a rapidity  $x_i$ , and the  $j$ -th vertical line a rapidity  $y_j$ . We restrict our attention to the fully inhomogeneous situation in which all rapidities are different.

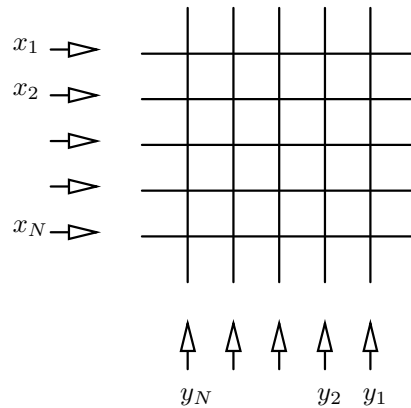


**Figure 3** The rapidity flows along the lattice lines. The direction of the flow is the orientation of the line. The strength of the flow is the rapidity. In our convention, the flow in each line orthogonally crosses lines with decreasing label.

**Bonds** are horizontal or vertical line segments that lies between two intersection points, or at the very end of a line.

**Arrows** To each bond we assign an arrow that can point in either direction along the bond.

**Vertices** We call the intersection point of the  $i$ -th horizontal line and the  $j$ -th vertical line, together with the 4 bonds attached to it, and the arrows on these bonds, a vertex  $v_{ij}$ .

This extends to the general case when the two intersecting lines are not ‘everywhere’ straight. The line orientations are sufficient to determine which of the two intersecting lines is ‘locally’ vertical and the other is ‘locally’ horizontal<sup>5</sup>.

**Weights** We assign each vertex,  $v_{ij}$ , a (Boltzmann) weight,  $W_{ij}$ , that depends on the following data

1. The orientations of the lines that intersect at that vertex. If necessary, we must rotate a vertex so that one line is oriented from left to right, while the other is oriented from bottom to top.
2. The orientations of the arrows on the four bonds attached to the intersection point.
3. The rapidities,  $\{x_i, y_j\}$ , flowing through the intersection point.
4. A parameter  $\lambda$ , called the crossing parameter that is the same for all vertices  $v_{ij}$ , and characterises the physical characteristics of the model.

**The six vertex model** Given that each vertex has 4 bonds, and each bond carries an arrow with 2 possible orientations, there are 16 possible vertex configurations. The six vertex model is the special case where only six types of vertices generally have non-zero weights. The weights of the remaining 10 types are set to zero. weights.

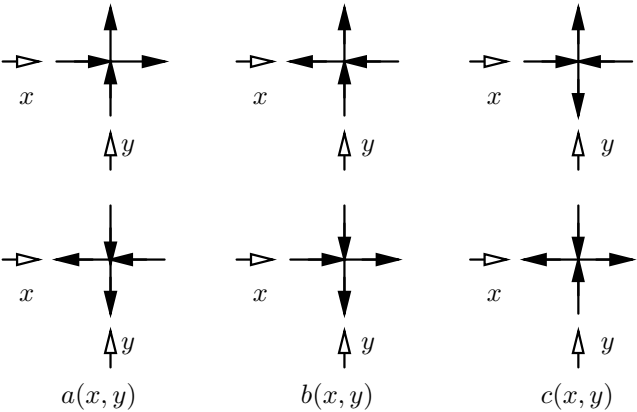


**Figure 4** The vertices of the six vertex model, with their rapidity flows. The weights of every two vertices in the same column are equal, and is shown below it.

<sup>5</sup>When in doubt, deform the intersecting lines locally such that their orientations agree with those given in figure 4.

**Conservation of arrow flow** The vertices with non-zero weights are precisely those that conserve arrow flow: In each vertex, two arrows point inwards, and two points outwards.

**Bracket notation** We define  $[x] = \sinh(\lambda x)$ , where  $\lambda$  is the crossing parameter.

**Vertex weights** In the bracket notation, the vertex weights are

$$a(x_i, y_j) = [-x_i + y_j + 1], \quad b(x_i, y_j) = [-x_i + y_j], \quad c(x_i, y_j) = [1] \quad (1)$$

where  $x_i$  (respectively  $y_i$ ) is the horizontal (respectively vertical) rapidity variable flowing through the vertex.

The weights of type  $a$  and type  $b$  vertices depend on the differences of the rapidities flowing through the vertex, and can vanish for specific values of the rapidities. The weight of the  $c$  vertex is independent of the rapidities.

**Yang Baxter equations** The origin of solvability of the six vertex model (irrespective of the boundary conditions) is that the (Boltzmann) weights of the model satisfy the Yang Baxter equations [1]. Defining the ( $R$ ) matrix

$$R(x, y) = \begin{pmatrix} a(x, y) & 0 & 0 & 0 \\ 0 & b(x, y) & c(x, y) & 0 \\ 0 & c(x, y) & b(x, y) & 0 \\ 0 & 0 & 0 & a(x, y) \end{pmatrix} \quad (2)$$

the set of all Yang Baxter equations can be written in matrix form as

$$R(x, y)R(x, z)R(y, z) = R(y, z)R(x, z)R(x, y) \quad (3)$$

where matrix multiplication is implied. The matrix equation 3 is equivalent to a set of equations between the weights. An example of a Yang Baxter equation, that will be used below, is shown graphically in figure 5.

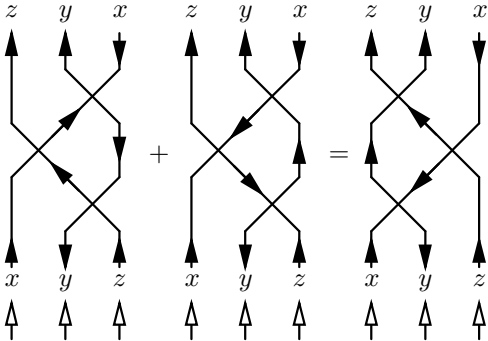


**Figure 5** A Yang Baxter equation. The external arrows, rapidities, and line orientations are the same on corresponding lines. Line orientations determine the vertex type unambiguously.

The Yang Baxter equation corresponding to figure 5 is

$$b(y, z)a(x, z)c(x, y) + c(y, z)c(x, z)b(x, y) = c(x, y)b(x, z)a(y, z) \quad (4)$$

**Domain wall boundary conditions (dwbc's)** For a vertex model on a finite square lattice, with  $N_c = N_r = N$ , one can require that all arrows on the left and right boundaries point inwards, and all arrows on the upper and lower boundaries point outwards. These are called ‘domain wall boundary conditions’ (dwbc’s)<sup>6</sup>. An example is shown in figure 6.

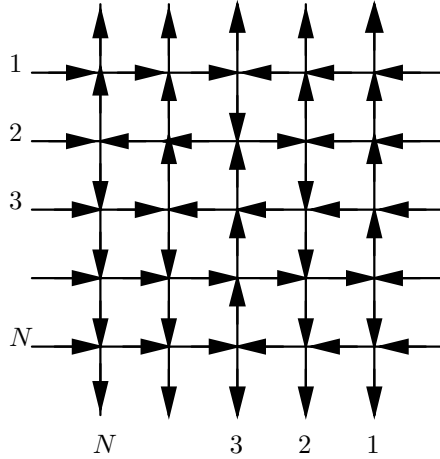


**Figure 6** A domain wall boundary configuration.

**Partition function** Given a statistical mechanical model, the partition function is defined as the sum over *all* weighted configurations. The weight of each configuration is the product of the weights,  $W_{ij}$ , of its vertices  $v_{ij}$

$$Z_N (\{x\}, \{y\}) = \sum_{\text{all allowed configurations}} \prod_{\text{vertices}} W_{ij} \quad (5)$$

**Remark 1** The expression in equation 5 is computationally worthless, as it cannot be evaluated in polynomial time in  $N$ .

## 2.1 Izergin’s expression for the partition function

In [3], Izergin solved Korepin’s recursion relations [2], and obtained an explicit expression for the partition function of the dwbc six vertex model in terms of a determinant

$$Z_N (\{x\}, \{y\}) = \frac{\prod_{i,j=1}^N a(x_i, y_j)b(x_i, y_j)}{\prod_{1 \leq i < j \leq N} b(x_i, x_j)b(y_j, y_i)} \det M$$

<sup>6</sup>One can equally well make the opposite choice of boundary arrow orientations. For consistency, we need to be make one choice and stay with that. This work is full of such choices.

$$= \frac{\prod_{i,j=1}^N [-x_i + y_j + 1] [-x_i + y_j]}{\prod_{1 \leq i < j \leq N} [-x_i + x_j] [-y_j + y_i]} \det M \quad (6)$$

where

$$M_{ij} = \frac{c(x_i, y_j)}{a(x_i, y_j)b(x_i, y_j)} = \frac{[1]}{[-x_i + y_j + 1] [-x_i + y_j]}$$

**Remark 2** *Izergin's expression, equation 6 for the partition function in terms of a determinant is computationally meaningful, as it can be evaluated in polynomial time in  $N$ .*

### 3 Correlation functions

Apart from the partition function which is the weighted sum over *all* configurations allowed by the dwbc's, one wishes to consider  $n$ -point correlation functions. These are defined as weighted sums over all configurations such that  $n$  arrows (that are summed over in the partition function) have certain frozen orientations.

Since the arrows on the outside of all vertical and horizontal lines are always frozen by definition of dwbc's, we need to consider freezing arrows that are on the inside of the lattice.

We start by considering the 1-point function obtained by summing all configurations such that a certain single arrow is kept frozen. Without loss of generality, let us consider freezing a horizontal arrow.

For example, consider freezing the orientation of the white arrow in figure 7, where bonds without arrows indicate bonds whose arrow orientations are summed over

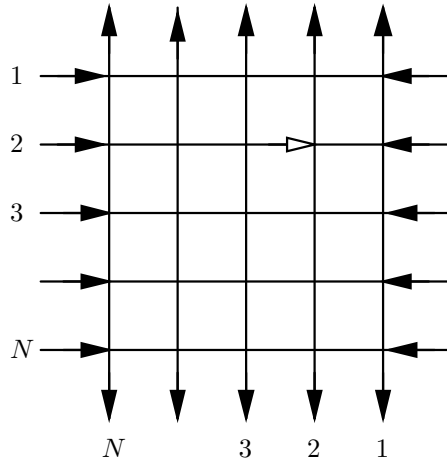


**Figure 7** *The configurations corresponding to a 1-point function.*

Our proposal is that one should start by slicing all such configuration into two parts, a right part, and a left part

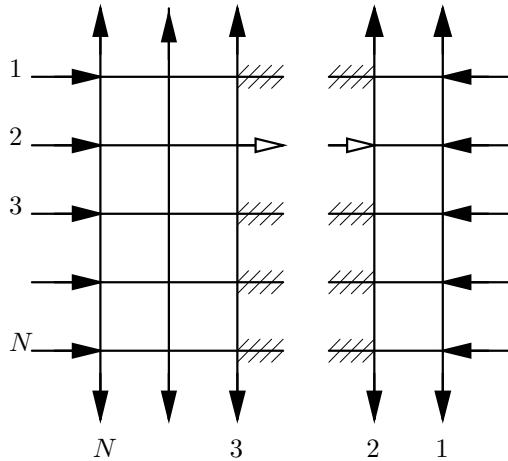


**Figure 8** *Slicing a domain wall configuration into two parts. The white arrows are frozen. The shaded exposed bonds indicate identified arrows that are summed over.*

where the dashed lines in figure 8 stand for bonds whose arrows are not frozen, and can take any orientation that is allowed.

**Exposed arrows** We call the arrows that were originally internal, and became external upon slicing the lattice, ‘exposed’ arrows. When we slice an  $N \times N$  lattice into two parts, there will be  $N$  exposed arrows on each part. The orientations of two exposed arrows that originate from slicing an originally internal bond are identical, and (generally) summed over.

**Boundary correlation functions** We wish to define each part, obtained by slicing a set of domain wall configurations, as in figure 8, as a boundary correlation function, with the understanding that arrows that were frozen by the original dwbc’s remain as they were,  $n$  exposed arrows (on each part) are frozen, the rest of the exposed arrows are summed over. In the example in figure 8,  $n = 1$ .

**Simple boundary  $n$ -point functions** There are special cases when *apart from* the  $n$  frozen arrows, the rest of the arrows assume domain wall boundary orientations: all those on the outside of the vertical boundary lines point inwards, and all those on the outside of the horizontal boundary lines point inwards. We refer to these as *simple  $n$ -point* boundary functions. For example, each part in the following set of configurations (with all internal arrows summed over) is a simple boundary 2-point function:



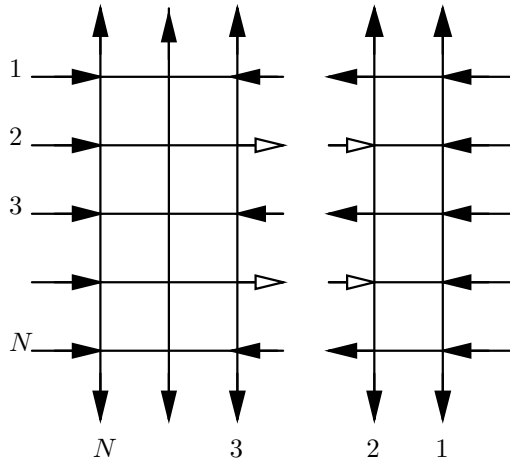


**Figure 9** *Two parts, each of which is a simple boundary 2-point function.*

**Origin of the simple boundary functions** From dwbc's, and conservation of arrow flow, there is exactly one horizontal arrow, pointing to the right, on the left of the right boundary, two such arrows to left of the second column, three to the left of the third, and so forth, until we reach the left boundary and find the correct dwbc's.

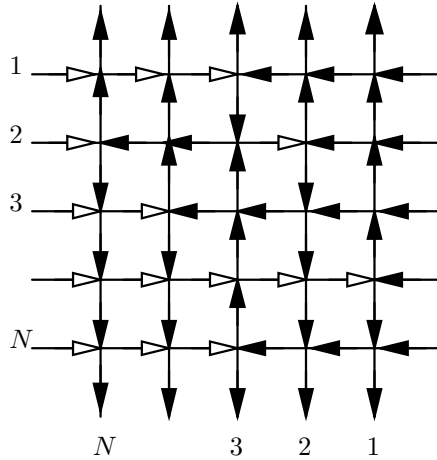


**Figure 10** *Scanning the white arrows from right to left, we can see how the number of horizontal arrows pointing to the right increases by 1, every time we step to the left.*

Simple  $n$ -point functions, with  $n$  horizontal arrows, all on the same column, are obtained by slicing a domain wall configuration vertically, between the  $n$ -th and vertical line (counting from the right) and the  $(n+1)$ -st line.

Precisely the same arguments apply to horizontal arrows that point to the left, and vertical arrows that point either up or down.

**Composite boundary  $n$ -point functions** are obtained, for example, when an  $N \times N$  lattice is sliced,  $N_{right}$  exposed arrows are pointing to the right,  $N - N_{right}$  are pointing to left, and we freeze  $n$  arrows that point, let's say, to the right. If  $n = N_{right}$ , then the boundary function is simple. If  $n < N_{right}$ , we need to sum over the positions of the remaining right-pointing arrows. Hence, such a boundary function is not simple.

**Bulk correlation functions** In principle, bulk  $n$ -point function, where all arrows point in the same direction, and lie on the same line, are obtained by taking products of boundary functions corresponding to each part.

More general bulk functions can be obtained by taking products of more general boundary functions. We have nothing deep to say about bulk functions at this stage.

## 4 Simple boundary 1-point functions

The simplest correlation function to compute is a simple boundary 1-point function. This will correspond to freezing any one of the white arrows shown in figure 11

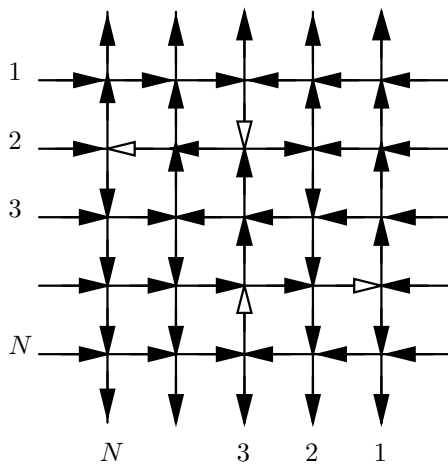


**Figure 11** *There is exactly one internal arrow, that touches a boundary, and that points opposite to the external arrows on the other side of that boundary.*

We choose to freeze the horizontal right-oriented arrow. Using the algebraic Bethe *ansatz*, Bogoliubov *et al* [5] obtained a determinant representation of this correlation function. More precisely, they obtained the partition function of the set of all domain wall boundary configurations such that the  $c$  vertex on the right boundary lies on row  $r$ , normalized by the full partition function  $Z_N$ . This is their definition of a boundary 1-point boundary function.

To reproduce their result, we start by slicing the lattice vertically, into two parts, and expose the frozen arrow

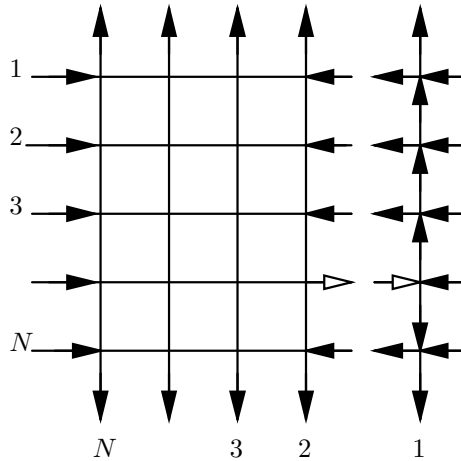


**Figure 12** *Slicing a domain wall configuration into two 1-point functions.*

We end up with *two* simple 1-point functions: One on the right, and one on the left. The right 1-point function is can be computed by inspection. The left will be computed below. The result of Bogoliubov *et al* is the product of the two parts, normalized by the partition function.

#### 4.1 The right boundary 1-point function

Consider the partition function of the  $1 \times N$  right part, and take the single  $c$  vertex to be on row  $r$ .

Given the dwbc's and conservation of arrow flows, all vertices that are above row  $r$ , will be of type  $b$ , all those below will be of type  $a$ , and the weight of the right part is

$$\left( \prod_{i=1}^{r-1} b(x_r, y_i) \right) c(x_r, y_1) \left( \prod_{i=r+1}^N a(x_i, y_1) \right) \quad (7)$$

#### 4.2 The left boundary 1-point function

Consider the partition function of the  $(N-1) \times N$  left part. If the inverted arrow on the right boundary were all the way at the top row, we would have the situation shown in figure 13.

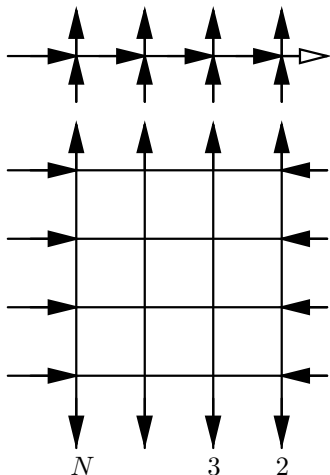


**Figure 13** ‘Peeling’ a frozen row.

In this case, all vertices on the top row are frozen to be of type  $a$ . Therefore, we can peel that top row, and end up with configurations on an  $(N-1) \times (N-1)$  square lattice that satisfy dwbc’s, and whose partition function can be evaluated using Izergin’s expression.

However, the inverted arrow is, in general, not at the top row. To bring it to the top row, we use the Yang Baxter equation as follows.

### 4.3 Rolling once

Consider the set of all configurations that remain after peeling the right boundary. They live on an  $(N-1) \times N$  lattice, with dwbc’s, except for an inverted arrow at row  $r$ , on the right boundary.

Take the inverted arrow to be (initially) at row  $i$ , and take the horizontal rapidity that flows through it to be (initially)  $x_i$ . We denote the partition function of the set of all such configurations by  $F[r_i, x_i]$ , and represent them schematically by the graph on the left hand side of figure 14.

Consider another set of configurations,  $F[r_{i-1}, x_{i-1}]$ , that is identical to  $F[r_i, x_i]$ , except that the inverted arrow is now on row  $r_{i-1}$ , and represent it schematically as the graph on the right in figure 14.

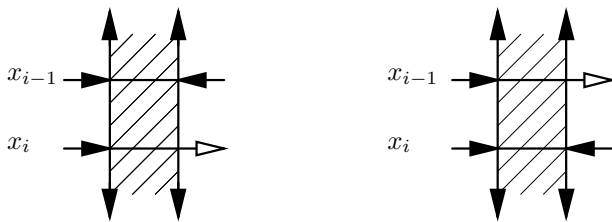


**Figure 14** The graph on the left is a schematic presentation of the set of configurations with an inverted arrow that we wish to roll upwards. The figure on the right is an identical set of configurations, apart from the fact that the inverted arrow is one row higher.

Multiplying the graph on the left by  $b(x_{i-1}, x_i)$ , and the graph on the right by  $c(x_{i-1}, x_i)$ , and adding the results

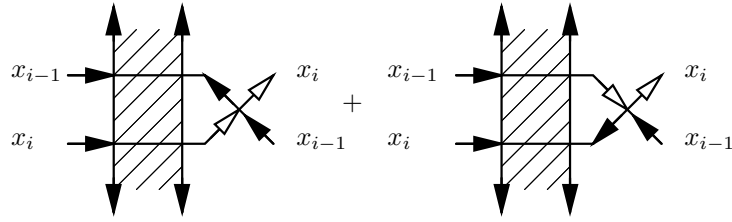


**Figure 15** *Multiplying the graph on the right by a type b vertex and that on the left by a type c vertex and adding the results.*

Since the arrows in the external loop on the right have both possible orientations, they are summed over, and we have

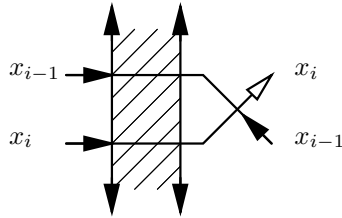


**Figure 16** *All possible arrow configurations that are allowed in the external loop on the right are summed over.*

But now we are in a position to use the Yang Baxter equation to move that external vertex, horizontally through the lattice, all the way to the left hand side

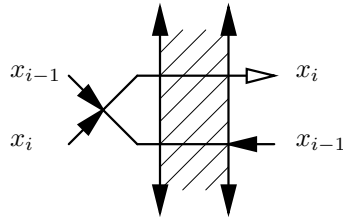


**Figure 17** *The result of using the Yang Baxter equation to weave the external loop all the way to the left. All possible arrow configurations in that loop are summed over.*

Given the orientations of the boundary arrows on the left hand side, the vertex that emerges is uniquely a type a vertex

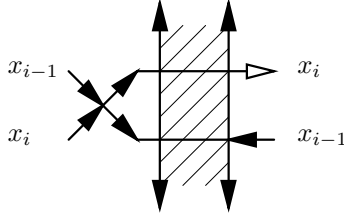


**Figure 18** *The only possible external vertex on the left is an a vertex.*

Equating the initial sum with the final result, we obtain

$$F[r_i, x_i]b(x_{i-1}, x_i) + F[r_{i-1}, x_{i-1}]c(x_{i-1}, x_i) = a(x_{i-1}, x_i)F[r_{i-1}, x_i] \quad (8)$$

Dividing both sides by  $b(x_{i-1}, x_i)$ , moving the second term on the left hand side to the right, and using  $b(x_i, x_{i-1}) = -b(x_{i-1}, x_i)$ , and  $c(x_i, x_{i-1}) = c(x_{i-1}, x_i)$ , we end up with the identity

$$F[r_i, x_i] = f(x_{i-1}, x_i)F[r_{i-1}, x_i] + g(x_i, x_{i-1})F[r_{i-1}, x_{i-1}] \quad (9)$$

where we have defined

$$f_{i,i+1} = \frac{a(x_i, x_{i+1})}{b(x_i, x_{i+1})}, \quad g_{i,i+1} = \frac{c(x_i, x_{i+1})}{b(x_i, x_{i+1})}$$

**Remark 3** *We write the weight of a type c vertex with formal dependence on its rapidities to make it easier to keep track of its position, although it is independent of the rapidities.*

Equation 9 says that we can rewrite the set of all configurations, in which the inverted arrow is on row  $i$ , in terms of configurations, in which the inverted arrow is in row  $(i-1)$ .

We have succeeded in ‘rolling’ the inverted arrow by one row towards the top. The price we have to pay for that is that we end up with two sets of configurations instead of one.

Further, it is easy to see that, if the initial inverted arrow is at row  $r$ , then rolling it upwards as we did above, the number of configurations will keep on doubling, leading to  $2^{r-1}$  configurations.

However, as we will see below, the Yang Baxter equation can be repeatedly used to reduce this number from  $2^{r-1}$  to  $r$ , which is typical of how the Yang Baxter equation makes models solvable [1].

To simplify the notation, we define

$$F_{i_1}^{i_2} = F[r_{i_1}, x_{i_2}] \quad (10)$$

as the configuration with the arrow on the  $i_1$ -th horizontal line inverted, and the rapidity through that line is  $x_2$ , so we have

$$F_i^i = f_{i-1,i}F_{i-1}^i + g_{i,i-1}F_{i-1}^{i-1} \quad (11)$$

#### 4.4 Rolling twice

Suppose we roll an inverted arrow up twice. From equation 11, we obtain

$$\begin{aligned}
F_i^i &= f_{i,i-1}F_{i-1}^i + g_{i-1,i}F_{i-1}^{i-1} \\
&= f_{i,i-1}(f_{i,i-2}F_{i-2}^i + g_{i-2,i}F_{i-2}^{i-2}) \\
&\quad + g_{i-1,i}(f_{i-1,i-2}F_{i-2}^{i-1} + g_{i-2,i-1}F_{i-2}^{i-2}) \\
&= f_{i,i-1}f_{i,i-2}F_{i-2}^i + f_{i-1,i-2}g_{i-1,i}F_{i-2}^{i-1} \\
&\quad + (g_{i-2,i}f_{i,i-1} + g_{i-1,i}g_{i-2,i-1})F_{i-2}^{i-2} \tag{12}
\end{aligned}$$

Equation 12 can be simplified by combining the two terms in the coefficient of  $F_{i-2}^{i-2}$  into one using a Yang Baxter equation as follows. Re-expand the coefficients of  $F_{i-2}^{i-2}$  in terms of Boltzmann weights to obtain

$$\begin{aligned}
g_{i-2,i}f_{i,i-1} + g_{i-1,i}g_{i-2,i-1} &= \tag{13} \\
\frac{c(x_{i-2}, x_i) a(x_i, x_{i-1})}{b(x_{i-2}, x_i) b(x_i, x_{i-1})} &+ \frac{c(x_{i-1}, x_i) c(x_{i-2}, x_{i-1})}{b(x_{i-1}, x_i) b(x_{i-2}, x_{i-1})} \tag{14}
\end{aligned}$$

Rewriting the right hand side of equation 13 in a slightly more convenient form, we obtain

$$\begin{aligned}
&\tag{15} \\
-\frac{c(x_i, x_{i-2}) a(x_i, x_{i-1})}{b(x_i, x_{i-2}) b(x_i, x_{i-1})} &+ \frac{c(x_i, x_{i-1}) c(x_{i-1}, x_{i-2})}{b(x_i, x_{i-1}) b(x_{i-1}, x_{i-2})} \tag{16}
\end{aligned}$$

Multiply both terms in equation 15 by

$$b(x_i, x_{i-1})b(x_i, x_{i-2})b(x_{i-1}, x_{i-2}) \tag{17}$$

we obtain

$$-a(x_i, x_{i-1})c(x_i, x_{i-2})b(x_{i-1}, x_{i-2}) + c(x_i, x_{i-1})c(x_{i-1}, x_{i-2})b(x_i, x_{i-2}) \tag{18}$$

Comparing equation 18 with the left hand side of the Yang Baxter equation 4, we find that they are identical, if we identify  $x \rightarrow i, y \rightarrow i-2, z \rightarrow i-1$ . Using these identifications, we can write equation 4 as

$$\begin{aligned}
c(x_{i-1}, x_{i-2})c(x_i, x_{i-1})b(x_i, x_{i-2}) &+ b(x_{i-2}, x_{i-1})a(x_i, x_{i-1})c(x_i, x_{i-2}) \\
&= c(x_i, x_{i-2})b(x_i, x_{i-1})a(x_{i-2}, x_{i-1}) \tag{19}
\end{aligned}$$

Dividing the right hand side of equation 19 by the expression in equation 17, we obtain

$$g_{i-2,i}f_{i,i-1} + g_{i-2,i-1}g_{i-1,i} = g_{i-2,i}f_{i-2,i-1}$$

So we end up with

$$F_i^i = f_{i,i-1}f_{i,i-2}F_{i-2}^i + f_{i-1,i-2}g_{i-1,i}F_{i-2}^{i-1} + f_{i-2,i-1}g_{i-2,i}F_{i-2}^{i-2} \tag{20}$$

## 4.5 Rolling many times

It is straightforward to iterate the above equation to bring the inverted arrow to the top. If the initial position is  $r$ , with rapidity  $x_r$ , we obtain

$$F_r^r = \sum_{\alpha=1}^{r-1} \left( g_{\alpha,r} \prod_{\substack{i=1 \\ i \neq \alpha}}^{r-1} f_{\alpha,i} \right) F_1^\alpha + \left( \prod_{i=1}^{r-1} f_{r,i} \right) F_1^r = \sum_{\alpha=1}^r \left( \frac{g_{\alpha,r}}{f_{\alpha,r}} \prod_{\substack{i=1 \\ i \neq \alpha}}^r f_{\alpha,i} \right) F_1^\alpha$$

where we have used

$$\frac{g_{r,r}}{f_{r,r}} = 1$$

Initially, we have the rows all labelled correctly, but the arrow on row  $r$  is inverted.

After rolling the inverted arrow (in the remaining lattice) to the top row, as we did above, the top row (which has  $n - 1$  vertices) is now ‘frozen’, in the sense that we know that all of its vertices are  $a$  vertices. Peeling these, we pick up a factor of

$$\prod_{j=2}^N a(x_k, y_j)$$

where  $x_k$  is the rapidity that ended at the top. The partition function of the remaining configurations can now be computed using Izergin’s expression. Putting all contributions together, we obtain

$$F_r^r = \sum_{\alpha=1}^r \left( \prod_{j=2}^N a(x_\alpha, y_j) \right) \left( \frac{g_{\alpha,r}}{f_{\alpha,r}} \prod_{\substack{i=1 \\ i \neq \alpha}}^r f_{\alpha,i} \right) Z_{N-1}(\underline{x}_\alpha, \underline{y}_1)$$

where  $Z_{N-1}(\underline{x}_\alpha, \underline{y}_1)$ , with underlined arguments, is Izergin’s partition function for an  $(N-1) \times (N-1)$  lattice, with the same assignment of horizontal and vertical rapidities, as those of  $Z_N(\{x\}, \{y\})$ , but with  $x_\alpha$  and  $y_1$  missing.

**The result of Bogoliubov, Pronko and Zvonarev** for the boundary 1-point function,  $H_N^r$ , in their definition, can be produced by multiplying the left and the right 1-point functions computed above, and normalising the product by the partition function of the  $N \times N$  model, to obtain

$$H_N^r(\{x\}, \{y\}) = \frac{1}{Z_N(\{x\}, \{y\})} \left( \prod_{i=1}^{r-1} b(x_r, y_1) \right) c(x_r, y_1) \left( \prod_{i=r+1}^N a(x_i, y_1) \right) \times \sum_{\alpha=1}^r \left( \prod_{j=2}^N a(x_\alpha, y_j) \right) \left( \frac{g_{\alpha,r}}{f_{\alpha,r}} \prod_{\substack{i=1 \\ i \neq \alpha}}^r f_{\alpha,i} \right) Z_{N-1}(\underline{x}_\alpha, \underline{y}_1) \quad (21)$$



## 4.6 Rolling down

It is possible to repeat the above exercise by rolling downwards, rather than upwards. The resulting expression will look different from that obtained above. In particular, the peeled rows will be products of  $b$  rather than  $a$  weights. We leave it as an (easy) exercise to the reader to show that the resulting expression is trivially equivalent to the first.

## 5 Simple boundary 2-point functions

We are now ready to extend the above arguments to simple boundary 2-point functions. There are four cases to consider:

1. The second inverted arrow is on the same boundary as the first.
2. The second inverted arrow is on one of the two boundaries adjacent (rather than opposite) to that of the first.
3. The second inverted arrow is on the opposite boundary to that of the first, but not directly opposite to it.
4. The second inverted arrow is on the opposite boundary to that of the first, and directly opposite to it.

Case 1 arises when an  $N \times N$  domain wall lattice is sliced into two parts with one part having  $2 \times N$  vertical (or horizontal) lines while the other part has the rest.

Cases 2, 3 and 4 arise in more complicated dissections of the original domain wall lattice (for example, into more than 2 parts). We deal with them for completeness.

### 5.1 Case 1

A non-trivial example of a simple 2-point function, with both inverted arrows on the same side, can be drawn schematically as follows

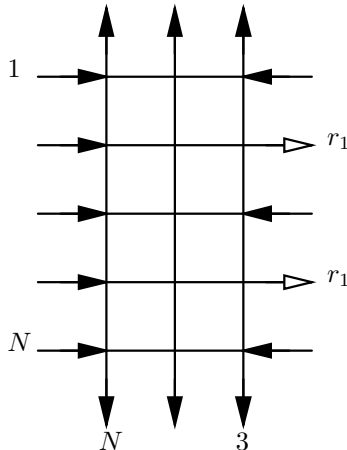


**Figure 19** A simple boundary 2-point function.

If the initial positions of the inverted arrows are  $r_1$  and  $r_2$ , where  $r_1 < r_2$ , with rapidities  $x_{r_1}$  and  $x_{r_2}$ , respectively, we can roll the upper arrow to the top, then roll the lower arrow to the row below the first, and obtain

$$F_{r_1, r_2}^{r_1, r_2} = \sum_{\alpha_1=1}^{r_1} \left( \frac{g_{\alpha_1, r_1}}{f_{\alpha_1, r_1}} \prod_{\substack{i_1=1 \\ i_1 \neq \alpha_1}}^{r_1} f_{\alpha_1, i_1} \right) \left( \prod_{j=3}^N a(x_{\alpha_1}, y_j) \right) F_{r_2}^{r_2}$$

and

$$F_{r_2}^{r_2} = \sum_{\substack{\alpha_2=2 \\ \alpha_2 \neq \alpha_1}}^{r_2} \left( \frac{g_{\alpha_2, r_2}}{f_{\alpha_2, r_2}} \prod_{\substack{i_2=2 \\ i_2 \neq \alpha_2}}^{r_2} f_{\alpha_2, i_2} \right) \left( \prod_{j=3}^N a(x_{\alpha_2}, y_j) \right) Z_{N-2}(\underline{x}_{\alpha_1}, \underline{x}_{\alpha_2}, \underline{y}_1, \underline{y}_2)$$

The full result is obtained by composing the above expressions. The extension of the above to  $(N-n) \times N$  lattices with  $n$  inverted arrows, all on the same boundary, is clear.

## 5.2 Case 2

In this case, there are two types of configurations to consider. In both types, we are dealing initially with an  $N \times N$  lattice. The first type can be drawn schematically as

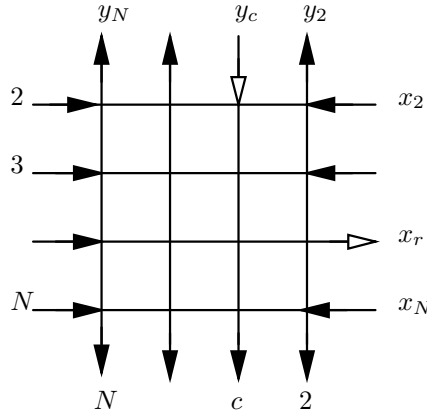


**Figure 20** A simple boundary 2-point function with inverted arrows on orthogonal boundaries.

In the second type, we consider a horizontal inverted arrow pointing to the right boundary, and a vertical inverted arrow pointing away from the lower boundary. Both types can be treated analogously (leading to analogous results with minor differences). In the following we will deal with the first and leave the second as an exercise to the reader.

If the positions of the inverted arrows are row  $r$  and column  $c$ , then we can write the result in two steps. First, we roll the inverted arrow on the right boundary all the way to the top to obtain<sup>7</sup>

<sup>7</sup>In this case there is no simple frozen upper row that can be peeled.

$$F_{cr}^{cr} = \sum_{\alpha=2}^r \left( \frac{g_{\alpha,r}}{f_{\alpha,r}} \prod_{\substack{i=2 \\ i \neq \alpha}}^r f_{\alpha,i} \right) F_{c1}^{c\alpha}$$

This leaves us with the factor  $F_{c\alpha}^{c1}$  corresponding to the lattice

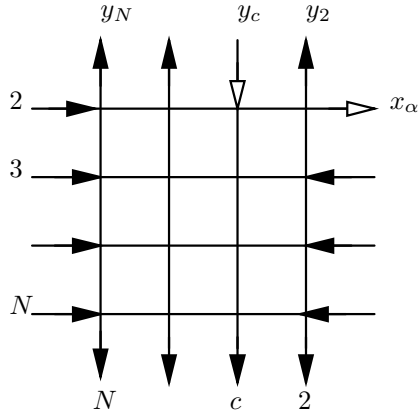


**Figure 21** *The right inverted arrow has been rolled all the way to the top.*

We need to roll the vertical inverted arrow all the way to the left. This can be done using exactly the same method that was used above to roll a horizontal inverted arrow to the top. In this case, we need to ‘inject’ an  $a$  vertex into the lattice from below and use the Yang Baxter equation to thread it all the way to the top. The result is exactly the same as in the case of horizontal arrows given that the extra vertex will move through the lattice in the same direction as the orientations of *both* vertical rapidities that end up swapping positions. The resulting configurations

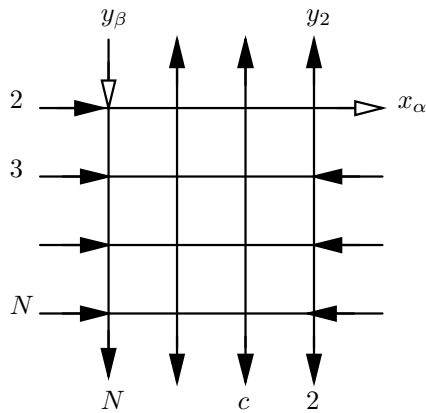


**Figure 22** *The upper inverted arrow has been rolled all the way to the left.*

can be evaluated by inspection to be

$$F_{c1}^{c\alpha} = \sum_{\beta=c}^N \left( \frac{\tilde{g}_{\beta,c}}{\tilde{f}_{\beta,c}} \prod_{\substack{j=c \\ j \neq \beta}}^N \tilde{f}_{\beta,j} \right) \left( \prod_{\substack{j=2 \\ j \neq \beta}}^{N-1} a(x_\alpha, y_j) \right) \left( \prod_{i=2}^N b(x_i, y_\beta) \right) \times \quad (22)$$

$$Z_{N-2}(\underline{x}_1, \underline{y}_1, \underline{x}_\alpha, \underline{y}_\beta) \quad (23)$$

where we have defined

$$\tilde{f}_{i,i+1} = \frac{a(y_i, y_{i+1})}{b(y_i, y_{i+1})}, \quad \tilde{g}_{i,i+1} = \frac{c(y_i, y_{i+1})}{b(y_i, y_{i+1})}$$

### 5.3 Case 3

This is a direct extension of case 1. We take the inverted arrows to be those on the right and left boundaries.

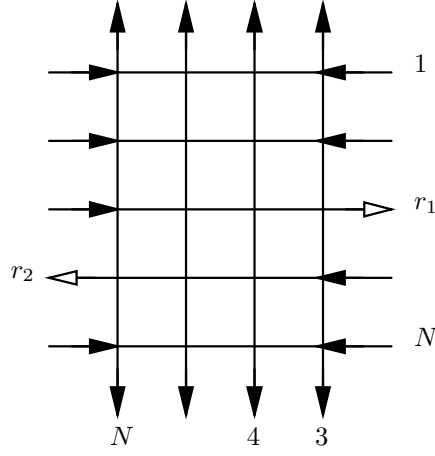


**Figure 23** A simple boundary 2-point function with inverted arrows on opposite boundaries, but not directly opposite to one another.

Rolling the higher inverted arrow, then the lower one, we end up with the configuration

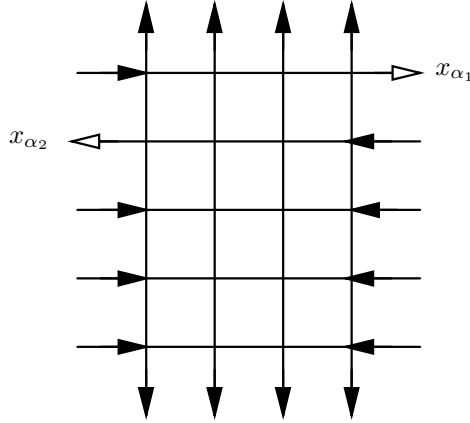


**Figure 24** *The inverted arrow have been rolled all the way to the top two rows.*

which can be evaluated by inspection to be

$$\begin{pmatrix} r_2 \\ r_2 \end{pmatrix} F \begin{pmatrix} r_1 \\ r_1 \end{pmatrix} = \sum_{\alpha_1=1}^{r_1} \left( \frac{g_{\alpha_1, r_1}}{f_{\alpha_1, r_1}} \prod_{\substack{i=1 \\ i \neq \alpha_1}}^{r_1} f_{\alpha_1, i} \right) \left( \prod_{j=3}^N a(x_{\alpha_1}, y_j) \right) \begin{pmatrix} r_2 \\ r_2 \end{pmatrix} F$$

where

$$\begin{pmatrix} r_2 \\ r_2 \end{pmatrix} F = \sum_{\substack{\alpha_2=2 \\ \alpha_2 \neq \alpha_1}}^{r_2} \left( \frac{g_{\alpha_2, r_2}}{f_{\alpha_2, r_2}} \prod_{\substack{i_2=2 \\ j \neq r_1}}^{r_2} f_{\alpha_2, i_2} \right) \left( \prod_{j=3}^N b(x_{\alpha_2}, y_j) \right) Z_{N-2} \left( \underline{x}_{\alpha_1}, \underline{x}_{\alpha_2}, \underline{y}_1, \underline{y}_2 \right)$$

where we have used a self-explanatory notation to indicate the position and rapidity labels of the inverted arrow on the left boundary.

#### 5.4 Case 4

In this case, we need to deal with inverted arrows that are directly opposite to each other.

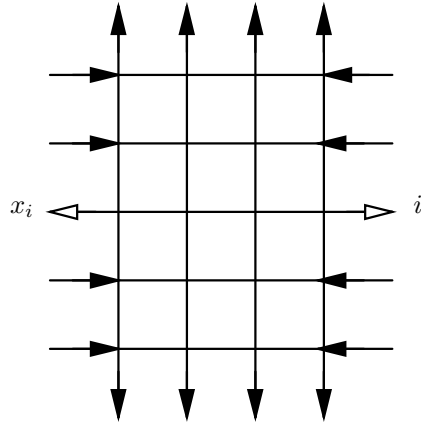


**Figure 25** A 2-point function with two inverted arrows on opposite boundaries, and directly opposite to one another.

It is clear that in this case, the above rolling argument needs to be slightly modified, as there is no way to multiply by an  $a$  weight from one side, and thread that to the other side to roll an inverted arrow.

We wish to show that this case can be reduced to a sum over cases of type 3, discussed above. Consider two configurations drawn schematically as follows (all external arrows that are not drawn are meant to be the same in both configurations, and all internal arrows are summed over)

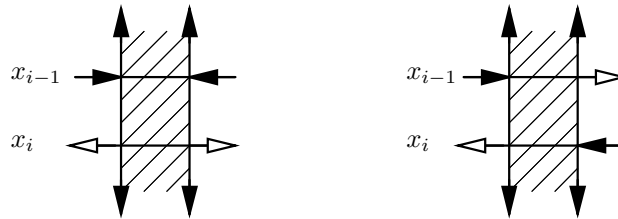


**Figure 26** The figure on the left is a schematic presentation of the set of configurations with directly opposite inverted arrows that we wish to roll up. The figure on the right is identical to the first, but the inverted arrow on the right is one row higher.

The configuration on the left is the one that we are interested in. The configuration on the right is auxiliary. Multiply the left configuration by a  $b$  vertex, the right configuration by a  $c$  vertex and consider the sum of the two results

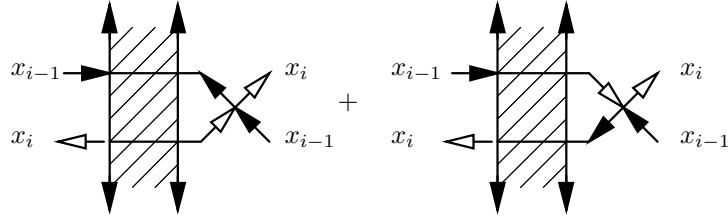


**Figure 27** *Multiplying the graph on the left above by a type b vertex, and that on the right by a type c vertex, and adding the results.*

In the sum, all internal arrows, in the external loop on the right, are now summed over, and the the sum can be represented in terms of the single graph on the left of equation 28 Applying the Yang Baxter equation to weave that external vertex through the lattice we obtain the graph on the right of figure 28

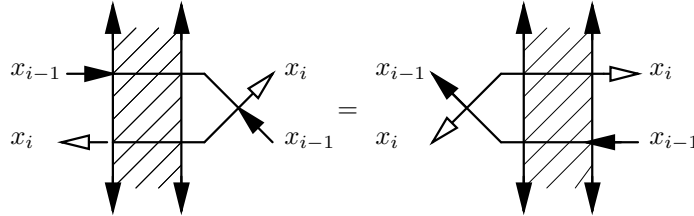


**Figure 28** *All arrow orientations that are allowed in the external loop on the right of the left figure are summed over, so we can use the Yang Baxter equation to weave that external vertex through the lattice from the right to the left.*

The resulting term on the right hand side of equation 28 can now be decomposed as

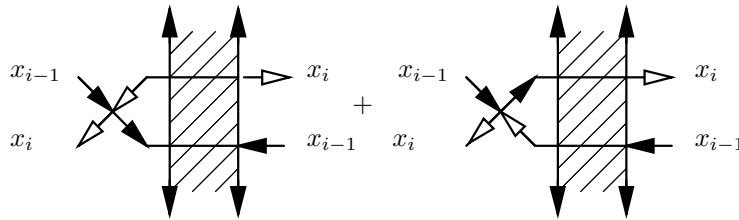


**Figure 29** *Showing the content of the arrow configurations of the external loop on the left.*

Dividing all terms by  $b(x_i, x_{i-1})$ , moving a term from the left hand side to the right, and using the antisymmetry of the  $b$  weights, we obtain

$$\binom{i}{i} F_i^i = \binom{i}{i-1} F_{i-1}^i + g_{i,i-1} \binom{i-1}{i} F_i^{i-1} + g_{i-1,i} \binom{i-1}{i} F_{i-1}^i \quad (24)$$

Equation 24 says that the problem with two opposing inverted arrow at row  $i$  can be reduced to the same problem at row  $(i-1)$ , plus two boundary 2-point functions of the type discussed in Case 3 above.

Using equation 24 repeatedly, boundary 2-point functions with opposite inverted arrows can be computed in terms of a sum boundary 2-point functions of type 3.

**Remark 4** *One can show by direct calculation that  ${}^2_1F_1^2$  vanishes, and hence*

$$\left( {}^2_2F_2^2 \right) = g_{2,1} \left( {}^1_2F_2^1 \right) + g_{1,2} \left( {}^1_2F_1^2 \right)$$

## 5.5 Boundary $n$ -point functions

**Simple boundary  $n$ -point functions** can be constructed almost mechanically by repeated application of the above arguments. All that is needed is to develop conventions to handle the notational complexity of the resulting expressions.

**Composite boundary  $n$ -point functions** will require summing over those inverted boundary arrows that are not frozen, which signals a proliferation of terms. However, there is hope that such summations can be simplified.

In [5], Bogoliubov *et al* evaluate not only boundary 1-point functions, but also *the boundary spontaneous polarizations* which are basically sums over many 1-point functions. Bogoliubov *et al* use the algebraic Bethe *ansatz* to obtain expressions that do not contain more terms than a typical 1-point function evaluated at the same point as the boundary spontaneous polarization.

This leads us to believe that sums that arise in computing ‘composite’ boundary  $n$ -point functions can also be performed, leading to relatively simple expressions.

## 5.6 Bulk correlation functions

It is clear how the bulk functions can be obtained as sums over products of boundary functions. In the simplest case of a 1-point function of a frozen arrow located deep in the lattice, the result is a product of two composite boundary correlation functions.

It is highly unlikely that such (typically large) sums over products can be used to deduce physical properties of correlation functions. To get manageable results, we need to develop efficient methods to evaluate the composite boundary functions, which brings us back to the comments made in the above paragraphs.

## 6 Epilogue

The point of this work was to show that the result of Bogoliubov *et al* can be reproduced using simple arguments. We also wished to show the same arguments apply, basically with no modification to higher simple boundary functions. The expressions that we obtain become cumbersome for higher  $n$ -functions, but they can be written basically by inspection of corresponding graph.

We hope that there are ways to simplify these expressions by performing suitable summations.



## Acknowledgements

O F wishes to thank J de Gier, M Jimbo and N Kitanine for discussions on this work and related topics. I P wishes to thank Mr Michael Watt for generously sponsoring his scholarship.

This research was supported by the Australian Research Council (ARC), and partially carried out while I P was visiting the Department of Mathematics and Statistics, The University of Melbourne.

## References

- [1] R J Baxter, *Exactly solved models in statistical mechanics*, Academic Press, 1982.
- [2] V E Korepin, *Commun. Math. Phys* **86** (1982) 391–418.
- [3] A G Izergin, *Sov. Phys. Dokl.* **32** (1987) 878–879.
- [4] V E Korepin, N M Bogoliubov, and A G Izergin, *Quantum inverse scattering method and correlation functions*, Cambridge University Press, 1993.
- [5] N M Bogoliubov, A G Pronko, and M B Zvonarev, *Boundary correlation functions of the six-vertex model*, *J Phys A: Math. Gen.* **35** (2002) 5525–5541.
- [6] G Kuperberg, *Another proof of the alternating sign matrix conjecture*, *Internat. Math. Res. Notices* (1996), No 3, 139–150.